Neuron

A prefrontal network integrates preferences for advance information about uncertain rewards and punishments

Highlights

- Little is known about the mechanisms of information seeking about punishments
- Attitudes toward information about uncertain punishments and rewards are separable
- ACC neurons anticipate information about either punishments or rewards
- vlPFC neurons reflect integrated preferences for both reward and punishment information

Authors

Ahmad Jezzini,
Ethan S. Bromberg-Martin,
Lucas R. Trambaiolli,
Suzanne N. Haber, Ilya E. Monosov

Correspondence

ilya.monosov@gmail.com

In brief

Despite its clinical and societal relevance, very little is known about how the brain regulates information seeking about aversive punishments. Here, the authors uncovered a prefrontal network, including the anterior cingulate and the ventral lateral prefrontal cortex, that tracks uncertainty and the motivation to seek information about uncertain rewards and punishments.

Jezzini et al., 2021, Neuron *109*, 2339–2352
July 21, 2021
https://doi.org/10.1016/j.neuron.2021.05.013

CellPress

Neuron

CellPress

Article

A prefrontal network integrates preferences for advance information about uncertain rewards and punishments

Ahmad Jezzini,[1] Ethan S. Bromberg-Martin,[1,8] Lucas R. Trambaiolli,[7,8] Suzanne N. Haber,[6,7] and Ilya E. Monosov[1,2,3,4,5,9,*]
[1]Department of Neuroscience, Washington University School of Medicine, St. Louis, MO 63110, USA
[2]Department of Biomedical Engineering, Washington University, St. Louis, MO 63130, USA
[3]Department of Electrical Engineering, Washington University, St. Louis, MO 63130, USA
[4]Department of Neurosurgery School of Medicine, Washington University, St. Louis, MO 63110, USA
[5]Pain Center, Washington University School of Medicine, St. Louis, MO 63110, USA
[6]Department of Pharmacology and Physiology, University of Rochester, Rochester, NY 14627, USA
[7]Basic Neuroscience, McLean Hospital, Harvard Medical School, Belmont, MA 02478, USA
[8]These authors contributed equally
[9]Lead contact
*Correspondence: ilya.monosov@gmail.com
https://doi.org/10.1016/j.neuron.2021.05.013

SUMMARY

Humans and animals can be strongly motivated to seek information to resolve uncertainty about rewards and punishments. In particular, despite its clinical and societal relevance, very little is known about information seeking about punishments. We show that attitudes toward information about punishments and rewards are distinct and separable at both behavioral and neuronal levels. We demonstrate the existence of prefrontal neuronal populations that anticipate opportunities to gain information in a relatively valence-specific manner, separately anticipating information about either punishments or rewards. These neurons are located in anatomically interconnected subregions of anterior cingulate cortex (ACC) and ventrolateral prefrontal cortex (vlPFC) in area 12o/47. Unlike ACC, vlPFC also contains a population of neurons that integrate attitudes toward both reward and punishment information, to encode the overall preference for information in a bivalent manner. This cortical network is well suited to mediate information seeking by integrating the desire to resolve uncertainty about multiple, distinct motivational outcomes.

INTRODUCTION

One of our most fundamental strategies for coping with an uncertain future is to seek information about what rewards and hazards the future holds. Indeed, humans and animals are often willing to pay to obtain information to resolve their uncertainty about future rewards, even when they cannot use this knowledge to change the outcome in any way (Blanchard et al., 2015; Bromberg-Martin and Hikosaka, 2009; Bromberg-Martin and Monosov, 2020; Eliaz and Schotter, 2007; Gottlieb et al., 2013; Kobayashi et al., 2019; Monosov, 2020; White et al., 2019). This non-instrumental preference for information about rewards is also reflected in the gaze behavior of monkeys and humans (Bromberg-Martin and Monosov, 2020; Daddaoua et al., 2016; Hunt et al., 2018; Monosov, 2020; Stewart et al., 2016; White et al., 2019). That is, when primates know that an object will provide a visual cue with information about future rewards, they are prone to hold their eye on that object in anticipation of viewing the cue and resolving their reward uncertainty as early as possible (White et al., 2019).

Taking advantage of these behavioral observations, the field is beginning to learn how the brain controls our desire to know what rewards our future holds (Bromberg-Martin and Monosov, 2020; Gottlieb et al., 2020; Monosov, 2020; Taghizadeh et al., 2020). For example, we found that the anterior cingulate cortex (ACC) contains a population of cells that predict reward-uncertainty-driven information-seeking behavior, and that ACC projection targets in the basal ganglia (BG) causally contribute to the motivation to make information-seeking eye movements (Bromberg-Martin and Monosov, 2020; Monosov, 2020; White et al., 2019). However, the cortico-cortical networks that participate with ACC in controlling information seeking are as of yet unknown.

In stark contrast with information seeking about uncertain rewards, very little is known about how the brain regulates information seeking about uncertain punishments (here defined as physically aversive or noxious outcomes). This is striking given how our individual strategies for coping with uncertain future punishments impact our everyday lives and society as a whole, depending on whether we eagerly seek knowledge or ''stick our heads in the sand'' to avoid knowledge about them.

Behaviorally, we know that humans show variability in their desire for non-instrumental information to resolve uncertainty about future punishments (Miller, 1987). In clinical settings, some human patients want to know if they are likely to suffer various debilitating diseases, while others choose to avoid or see little value in obtaining this information prior to possible symptoms (Lerman et al., 1998; Miller, 1995). Relatedly, humans display variability in their curiosity to experience noxious stimuli and negatively valenced information in the form of aversive or scary images (Niehoff and Oosterwijk, 2020; Oosterwijk, 2017; Oosterwijk et al., 2020). Similarly, even humans who seek information about uncertain monetary gains can do so less consistently for uncertain monetary losses (Charpentier et al., 2018). Attitudes toward information about future punishments have also been investigated in animal models (Badia et al., 1979; Fanselow, 1979; Miller et al., 1983; Tsuda et al., 1989). However, the neuronal basis of these preferences remains unclear, because there has been no investigation of what neurons generate this preference and what neuronal code they use to do so. Furthermore, information preferences for punishments and rewards have predominantly been studied in isolation from each other (Bromberg-Martin and Monosov, 2020; Monosov, 2020), so little is known about whether and how attitudes toward these two types of information are linked to each other, at both the behavioral and neuronal levels.

To address these open questions, we designed an experiment to simultaneously measure the behavioral attitudes of monkeys toward information about punishments and rewards and investigated the prefrontal cortical substrates of these preferences. We discovered that attitudes toward punishment and reward information are not strictly tied to each other: individuals with similar preferences for reward information can have strikingly different attitudes toward punishment information. Furthermore, the ACC, as well as an anatomically interconnected subregion of the ventrolateral prefrontal cortex (vlPFC), contained neural populations that anticipated opportunities to gain uncertainty-resolving information in a valence-specific manner—anticipating information about either uncertain punishments or uncertain rewards. Crucially, vlPFC also contained a subpopulation of neurons that integrated attitudes toward punishment and reward information, consistent with encoding the overall preference for information in a bivalent manner suitable for guiding motivation and behavior. Indeed, neural information signals in both ACC and vlPFC reflected individual differences in the monkeys' preferences for the corresponding types of information, and trial-by-trial fluctuations in neural signals anticipating punishment information predicted the strength of information-anticipatory behavior. These results uncover a cortical network well suited to mediate information seeking to reduce uncertainty in a flexible manner by integrating distinct motivational outcomes.

RESULTS

Information preferences to resolve punishment and reward uncertainty are dissociable in individual animals

To study the mechanisms of information seeking and preference, we trained monkeys to associate visual fractal cues with different probabilities that a juice reward or air puff punishment would be delivered in the future (Figure 1A). The first visual fractal cue indicated the initial probabilities that rewards and punishments would be delivered in 3.25 s (Figure 1A, Cue1, "Initial prediction"). This included reward-predictive cues associated with 25%, 50%, 75%, and 100% probabilities of reward; punishment-predictive cues associated with 25%, 50%, 75%, and 100% probabilities of punishment; a neutral cue that was not followed by either punishment or reward; and a bivalent cue associated with a 50% chance of reward and a 50% chance of punishment (Figure 1B). This design allowed us to dissociate between high expectations of reward and punishment (maximal at 100%) and high amounts of uncertainty about reward and punishment (maximal at 50%) (Monosov, 2017; White et al., 2019; White and Monosov, 2016).

Crucially, this initial cue (Cue1) was always followed after 1 s by a second visual fractal cue, which could either provide additional information to resolve uncertainty about the outcome or could provide no new information (Figure 1B, Cue2, "Info or noinfo"). Thus, the identity of Cue1 indicated both the probabilities of reward and punishment and indicated whether the upcoming Cue2 would provide information about the outcome (Figure 1B). Specifically, an information-predictive Cue1 was always followed by an informative Cue2 that provided complete and accurate information about whether the trial's outcome would be a punishment, a reward, or neither (Figure 1B). A non-information-predictive Cue1 was always followed by a non-informative Cue2 whose identity was randomized and hence uncorrelated with the upcoming outcome (Figure 1B).

These two trial types were presented in separate blocks (Figure 1B, "Informative block" and "Non-informative block"). After training on the task, both monkeys had stable conditioned responses indicating that they learned the meanings of the task stimuli, by updating their predictions about rewards and punishments using both Cue1 and the informative Cue2s (Figure S1).

To test how these outcome predictions translated into behavioral preferences during decision making, we allowed monkeys to choose between all possible pairs of Cue1s in a two-alternative forced choice task (Figure 1C). We then used logistic regression to model their log odds of choosing each Cue1 as a linear weighted combination of its attributes, including its information predictiveness, its reward and punishment probabilities, and its reward and punishment uncertainties (operationalized here as their standard deviations) (Figure 1C). These attributes were chosen to replicate previous work on information seeking and risk seeking, to show that the animals understood the stimuli and assigned negative subjective values to punishments and positive subjective values to rewards, and to measure their attitudes toward reward-related and punishment-related uncertainty resolution. This allowed us to measure how animals subjectively valued the alternatives and, in particular, whether and how they valued information to resolve uncertainty about future outcomes.

The results corroborated our analysis of conditioned responses and were consistent with previous studies (Figure 1C). As expected, the choices of both monkeys were best fit by significant positive weights for reward probability and negative weights for punishment probability; i.e., monkeys were reward seeking and punishment averse. Also, as expected, both monkeys were fit with significant positive weights for reward

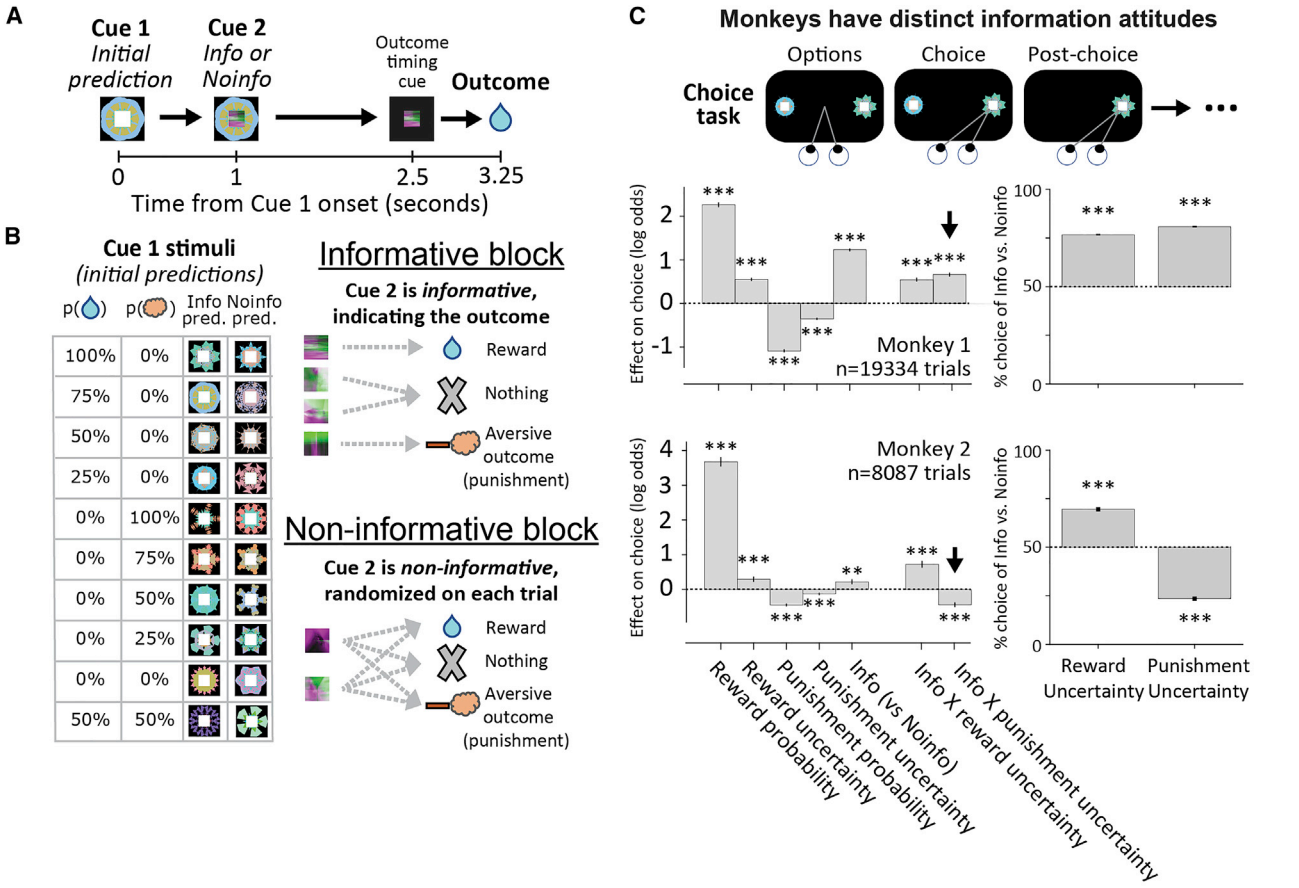

ACC subregions enriched with neurons anticipating the resolution of reward uncertainty are connected with vlPFC

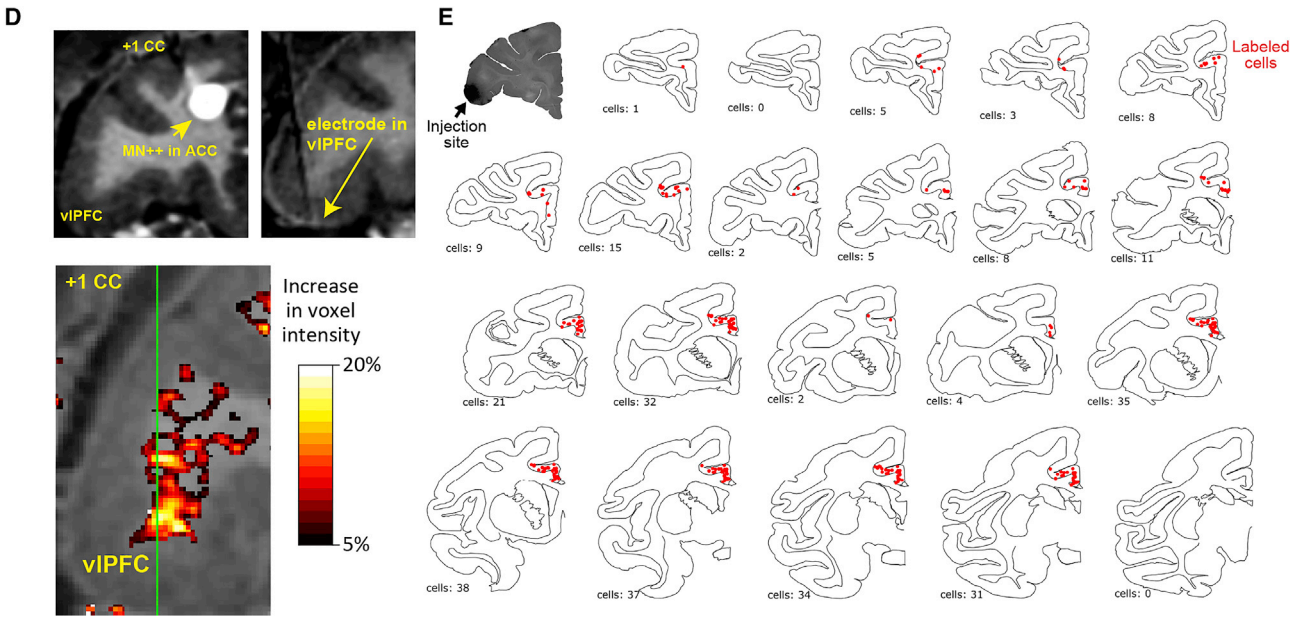

(legend on next page)

uncertainty; i.e., they were risk seeking for rewards (Christopoulos et al., 2009; Ledbetter et al., 2016; McCoy and Platt, 2005; Monosov, 2020; So and Stuphorn, 2010). We also found that both monkeys were fit with significant negative weights for punishment uncertainty. This demonstrates that monkeys have attitudes toward punishment uncertainty and specifically indicates that they can be risk averse for punishments. Finally, both monkeys were fit with significant positive weights for informativeness, indicating a general preference for advance information about future outcomes.

We next asked the key behavioral questions of our experiment: (1) Do monkeys have behavioral attitudes toward gaining information to resolve punishment uncertainty? (2) If so, what is the nature of their attitudes? That is, do they seek or avoid information about punishments? (3) What is the relationship between attitudes toward information about punishments and rewards? One hypothesis is that attitudes toward information are generated by the same neural algorithm for all types of uncertain motivational outcomes (for instance, by a neural process that follows the convention of many reinforcement learning models of simply treating punishments as "negative rewards"; Sutton and Barto, 1998). If so, then attitudes toward information about rewards and punishments should move in lockstep with each other. Alternately, attitudes toward information about rewards and punishments could be generated by distinct neuronal processes. In that case, they might also be dissociable at the level of behavioral preferences.

To answer these questions, we examined the model's weights for the interactions between informativeness and outcome uncertainty (Figure 1C, right). In other words, how did the preference for information scale with outcome uncertainty? This produced a striking dissociation. For rewards, both animals had a significantly greater preference for information for outcomes with a high degree of reward uncertainty (Figure 1C, info × reward uncertainty; Figure S2). For punishments, however, the two animals behaved quite differently from each other, with distinct and actually opposite informational preferences. Monkey 1 was best fit with a significant positive weight for the corresponding interaction term in the model, indicating that its information preference was enhanced by punishment uncertainty (Figure 1C, info × punishment uncertainty). In contrast, monkey 2 was best fit with a significant negative weight, indicating that its information preference was reduced by punishment uncertainty (Figure 1C). Importantly, their different attitudes toward obtaining information to resolve punishment uncertainty were not due to the animals having different attitudes toward encountering punishment uncertainty per se; both animals were best fit with significant negative weights of punishment uncertainty (Figure 1C). We observed similar results when examining raw choice percentages: on trials where both options had punishment uncertainty but only one option provided information, monkey 1 was significantly more likely to choose the informative option (information seeking), while monkey 2 was more significantly likely to choose the non-informative option (information averse) (Figure 1C, right). Furthermore, both monkeys' information preferences were significantly stronger for uncertain outcomes than certain outcomes, consistent with the hypothesis that their information preferences were motivated to resolve uncertainty (Figure S2). Also, their distinct preferences were not due to the information having any distinct objective, instrumental use in preparing for the air puffs (Figure S1). Thus, the behavior of these animals was consistent with observations in humans showing that some individuals cope with uncertain future punishments by seeking information about them, while others purposefully avoid information (Charpentier et al., 2018; Lerman et al., 1998; Miller, 1987, 1995).

Thus, these data answer the three key questions posed above: (1) monkeys can have strong attitudes toward gaining information to resolve punishment uncertainty; (2) the nature of their information attitude varies across individuals and can consist of either preferences or aversions; and (3) attitudes toward information about punishments and rewards are distinct and strongly dissociable, such that an individual animal's attitude toward the former can even be opposite to their attitude toward the latter.

Given this behavioral dissociation between attitudes toward information to resolve uncertainty about rewards versus punishments, we hypothesized that these preferences are generated by dissociable neural mechanisms. To test this idea, we build on a recent finding that information seeking to resolve reward uncertainty is controlled by a population of neurons that anticipatorily ramp toward the time of uncertainty resolution (Bromberg-Martin and Monosov, 2020; Monosov, 2020; White et al., 2019). These information preference-related neurons were found in the ACC and

Figure 1. Investigating information seeking to resolve uncertainty about rewards and punishments

(A) Timeline of events in the reward and punishment information task.

(B) In the informative block, 10 cues (Cue1s) yield 10 different chances of reward and punishment (air puffs) and are followed by informative cues (Cue2s) that indicate the outcome. In the non-informative block, 10 other cues (Cue1s) yield the same outcome probabilities but are followed by non-informative cues (Cue2s) that do not predict the outcome, so uncertainty is not resolved until outcome delivery.

(C) Choice version of the task. After choosing Cue1, the same sequence of events occurred as in the non-choice task (including Cue2, the pre-outcome timing cue, and the outcome). Plotted are the weights from a logistic regression fit to each monkey's choices based on the attributes of each Cue1, including outcome probability, uncertainty (operationalized as standard deviation), information-predictiveness, and key interactions. Both monkeys were fit with similar patterns of weights, including positive weights of info × reward uncertainty, with a key exception: monkey 1 had a positive weight of info × punishment uncertainty, while monkey 2 had a negative weight (black arrows). Error bars are ±1 SE. $^{**}p < 0.01$, $^{***}p < 0.001$. Right: % choice of informative versus non-informative Cue1 for trials where both options had reward uncertainty only (left bar) or punishment uncertainty only (right bar).

(D) Top left: 150-μl injection of manganese chloride anterograde tracer into the ACC region of monkey 1 that was enriched in information-anticipating neurons (White et al., 2019). Bottom left: % increase of voxel intensity (MEMRI labeling) shown in a coronal plane 24 h after injection in the vlPFC. Color axis: greater or equal to 20% change is shown as white, while black represents 5%. Top right: MRI with an electrode in monkey 1 targeting the MEMRI-identified region of vlPFC.

(E) Schematic chartings of the distribution of retrogradely labeled cells (red dots) in the ACC, areas 32 and 24, after LY injection in the vlPFC, area 12/47. Top left: the vlPFC tracer injection was placed in a similar location to the vlPFC electrode in (D). A cluster of labeled cells is observed over the same subregion injected with $Mn2^{+}$ in the ACC.

in specific regions of the BG that receive strong projections from the ACC. We previously found that the ACC had a particularly important role in this cortical-BG circuit. Both ACC and BG neurons predicted future information-seeking behaviors, but ACC neurons did so early in advance, while BG neurons did so only just before the behavior was carried out. Hence we hypothesized that the ACC may interact with other prefrontal regions to control information preference before the BG translates information preference into the motivation to act.

Anterior cingulate regions enriched with information-anticipating neurons form an anatomical network with the vlPFC

To identify regions that receive particularly strong inputs from the ACC, we turned to manganese-enhanced magnetic resonance imaging (MEMRI) (Monosov et al., 2015; Murayama et al., 2006; Saleem et al., 2002; Simmons et al., 2008). Ours and others' studies indicate that MEMRI reliably detects major outputs of regions injected with manganese chloride (Monosov et al., 2015; Murayama et al., 2006; Saleem et al., 2002; Simmons et al., 2008). We utilized MEMRI to identify candidate regions for receiving information-related signals from the ACC. To this end, we electrophysiologically identified a region within the ACC of one of our animals that was particularly enriched in neurons that anticipated reward uncertainty (Figure 1D) and injected it with manganese chloride. Subsequent magnetic resonance (MR) imaging (MRI) and analyses revealed several hotspots receiving ACC inputs. Consistent with our recent work, one hotspot was the internal capsule bordering dorsal striatum (icbDS; Figure S3A), a region that we previously identified as an anatomical target of ACC projections (Figure S3B) and as a key site of BG neural signals that anticipate information about uncertain future rewards (White et al., 2019).

A second hotspot was the vlPFC, especially areas 47/12, where intense MR signal was observed (Figure 1D). We sought to confirm this result, because MEMRI is not as precise as classical anatomical methods and can miss diffuse or weak projections (Monosov et al., 2015; Murayama et al., 2006; Saleem et al., 2002; Simmons et al., 2008). We therefore turned to retrograde and anterograde tracing. We injected retrograde tracer into the area of the vlPFC that received strong MEMRI-identified inputs from the ACC. This produced robust labeling in the ACC (Figure 1E), particularly in the same regions that we identified as enriched with information-related neurons (Monosov, 2017; White et al., 2019). Additional analyses of tracer injections confirmed the bidirectional nature of the ACC-vlPFC circuit (Figure S4). In addition, analysis of retrograde tracer injection into the BG confirmed that both ACC and vlPFC project to the same region of icbDS that contains activity anticipating information about uncertain rewards (Figure S3).

Single ACC and vlPFC neurons anticipate information to resolve reward and punishment uncertainty

We next used targeted electrophysiology to examine how the ACC and vlPFC participate in information seeking to resolve reward and punishment uncertainty. We studied task-sensitive neurons (Kruskal-Wallis test; $p < 0.01$; STAR Methods) in the ACC and vlPFC of the same monkeys whose behavior was shown in Figure 1 while they participated in the task in Figure 1A (M1 ACC: n = 149, vlPFC: n = 259; M2 ACC: n = 128, vlPFC: n = 275). We then quantified how single neurons responded to uncertainty about rewards and punishments, and whether they anticipated information to resolve that uncertainty.

We defined neural signals that anticipated information to resolve uncertainty as activity that (1) selectively differentiated task epochs when outcomes were uncertain versus certain and (2) was enhanced when animals were anticipating information that would resolve that uncertainty. Information anticipation was therefore indexed by neural signals that were enhanced on uncertain information trials in a time window immediately before the informative cue appeared (White et al., 2019).

We found that both ACC and the vlPFC contained single neurons that anticipated information to resolve reward or punishment uncertainty. An example of one such ACC neuron is shown in Figure 2A. In the informative block, the neuron was most strongly excited by Cue1 associated with punishment uncertainty (Figure 2A, top, red rasters and curves indicating 25%, 50%, and 75% chance of air puff > black rasters and curves indicating 0% and 100% chance of air puff). This uncertainty signal was strongest just before the informative cue appeared to resolve the uncertainty and then rapidly diminished afterward. In contrast, during the non-informative block, the same neuron did not discriminate between certain versus uncertain punishment predictions in advance of the non-informative cue. Furthermore, this neuron showed this information-anticipatory activity only for punishments; it had no similar anticipation of informative cues about uncertain rewards. Therefore, this neuron selectively anticipated the resolution of punishment uncertainty, but not reward uncertainty.

Although some neurons anticipated information about only one type of outcome (see additional example neurons in Figure S5), other neurons anticipated information about both punishments and rewards. This can be seen in a second example neuron from the vlPFC (Figure 2C). During the informative block, this neuron was activated by both punishment and reward uncertainty in similar manners. This signal was particularly strong in the moments before the informative cue appeared and then rapidly diminished after the cue appeared and resolved the uncertainty. During the non-informative block, the same neuron had little or no discrimination between certain versus uncertain outcome predictions in advance of the non-informative cue.

To quantify this selective information anticipation signal on a neuron-by-neuron basis, we followed the approach from White et al. (2019). We first computed an index quantifying the strength of uncertainty signals at each time during the task, using the receiver operating characteristic (ROC) area for discriminating neural activity from uncertain trials versus certain trials. We then computed this uncertainty index in a time window before Cue2 onset and calculated the difference between the index on trials where that cue was informative versus non-informative. This analysis is illustrated for the example neurons in Figures 2B and 2D. This approach identifies neurons with selective uncertainty signals that are stronger in anticipation of informative cues than non-informative cues.

Using this approach, we next asked two key questions: (1) Is information to resolve reward and punishment uncertainty generally anticipated in similar manners and by the same neural

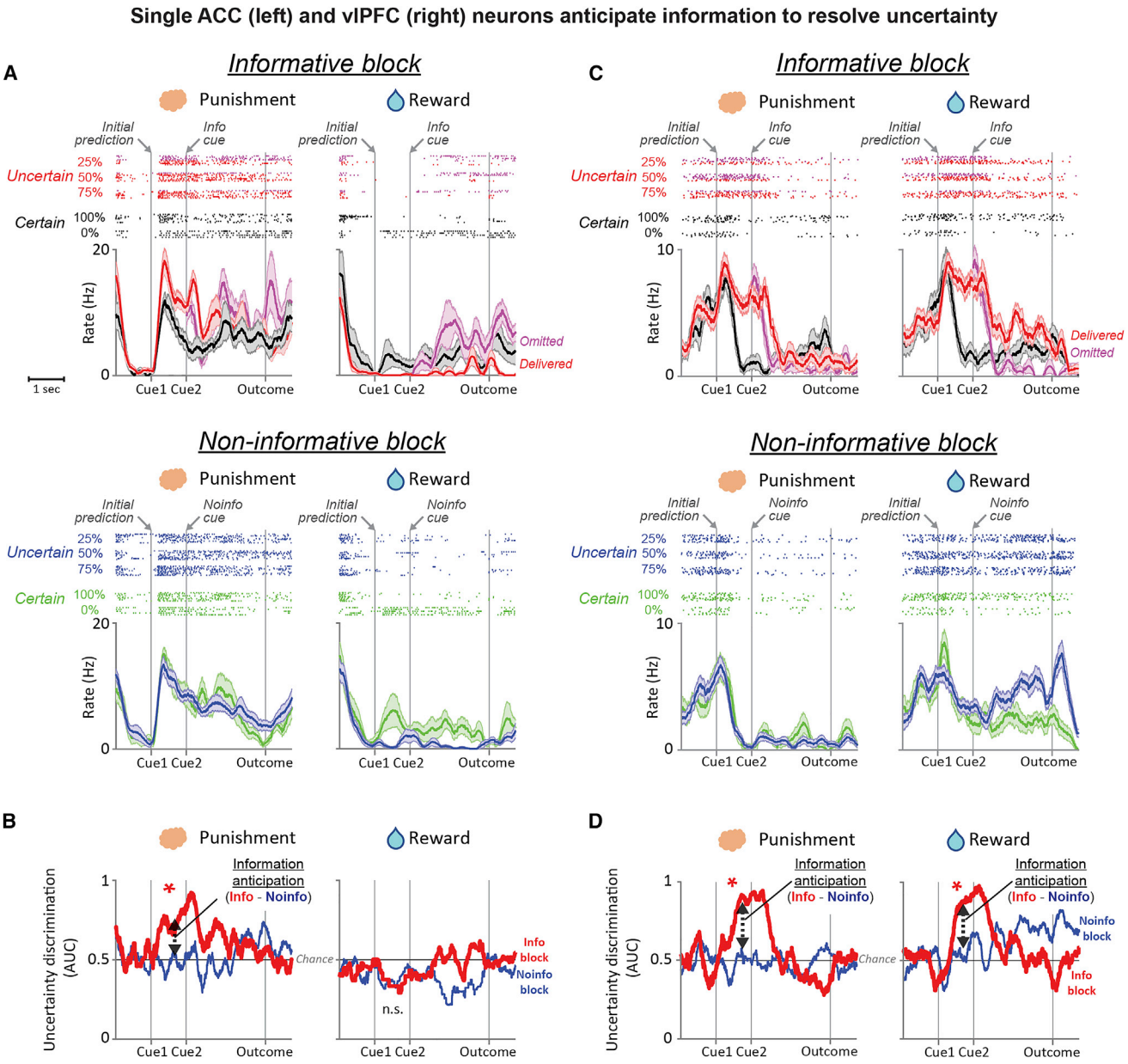

Figure 2. Example single ACC and vlPFC neurons that anticipate information to resolve uncertainty

(A and B) A single ACC neuron anticipates information to resolve punishment uncertainty. (A) Activity is shown separately for the informative and non-informative blocks (top, bottom), for punishment and reward trials (left, right), and for certain versus uncertain outcomes (colored rasters and spike density functions). Shaded area is SEM. After informative cues, activity is split into trials when outcomes were going to be delivered or omitted (red, magenta). (B) Information anticipation index displayed in time. During punishment trials, the uncertainty signal increases in anticipation of the informative cue that will resolve the monkey's uncertainty (red), but not in anticipation of non-informative cues (blue). The information anticipation index is quantified as the difference between uncertainty signals before onset of informative versus non-informative cues (Cue2) (* indicates $p < 0.05$; STAR Methods). The uncertainty signal (y-axis) is defined as the area under the curve (AUC) of the ROC for discriminating uncertain from certain trials.

(C and D) A single vlPFC neuron anticipates information to resolve uncertainty about both punishments and rewards. Same format as (A) and (B).

population, or is it anticipated by distinct populations? And is this the same in ACC and vlPFC? (2) Are there significant differences in the neural codes of these populations reflecting individual differences in information attitudes, especially their attitudes toward information about uncertain punishments, which were strikingly different between animals?

Information-seeking preferences are reflected in distinct manners across the ACC-vlPFC network

We found that in both monkeys, many task-responsive ACC neurons significantly anticipated reward information, and the proportion of these neurons was much greater than would be expected by chance (Figures 3A–3B, left, binomial test, $p < 10^{-6}$ in

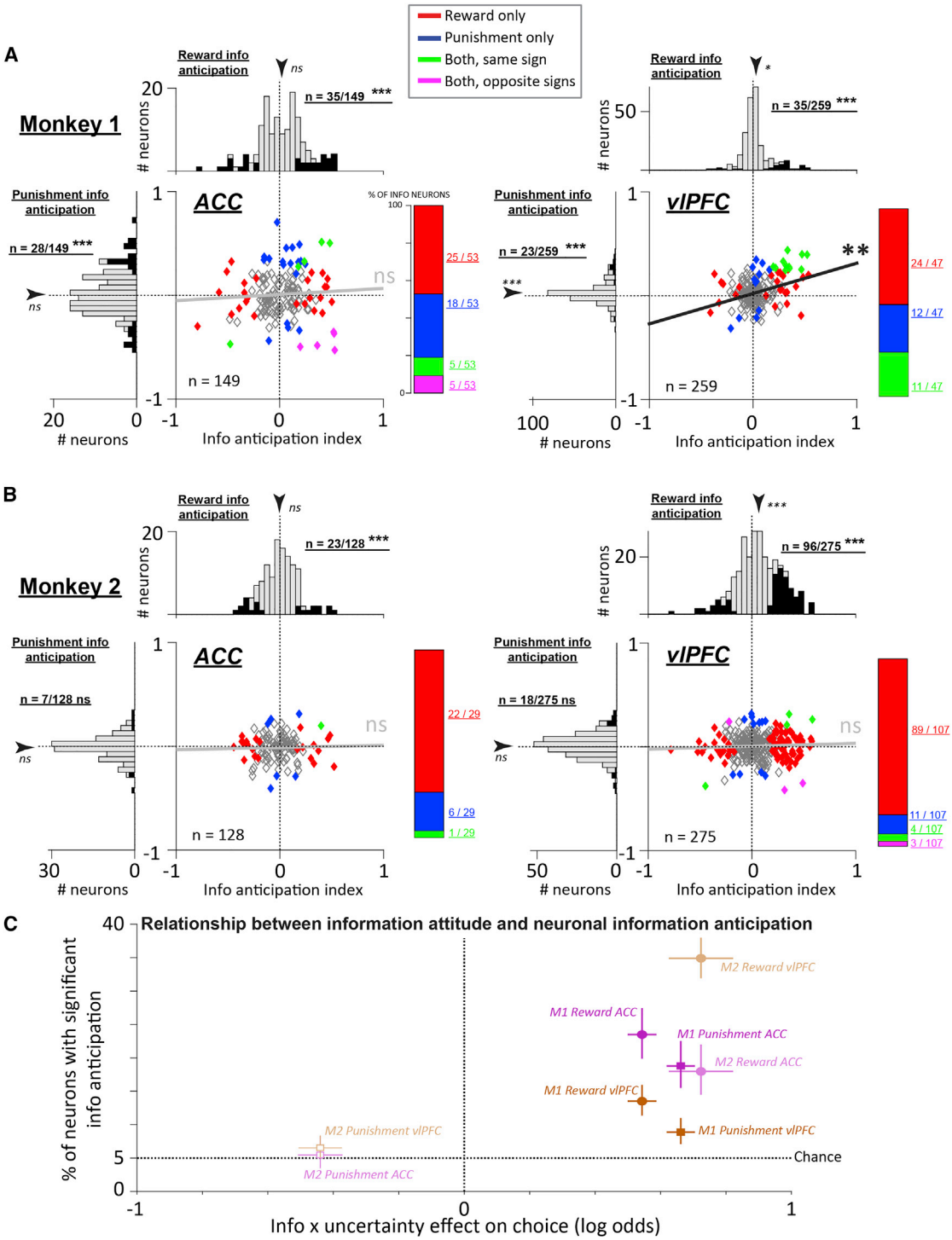

Figure 3. ACC and vlPFC neurons anticipate information to resolve uncertainty about rewards and punishments and reflect information attitudes

(A) Neural information anticipation indexes for resolving uncertainty about rewards and punishments (x- and y-axes) in monkey 1. Each data point is a neuron in the ACC (left) or vlPFC (right). Colors indicate neurons that significantly anticipate information to resolve uncertainty about punishments (blue), rewards (red), both with the same coding sign (green), or both with opposite coding signs (magenta). To the right of each scatter, a bar plot shows the relative proportions of these groups. Marginal histograms summarize the single neuron indexes. Arrow is the mean, and asterisks indicate significance if the median is different from 0 (signed-rank test). Filled bars indicate significant neurons, and the text next to each marginal histogram indicates whether that number of neurons is significantly more than expected by chance (binomial test). Both ACC and vlPFC had significant numbers of neurons anticipating information to resolve reward and punishment

(legend continued on next page)

both animals). In monkey 1, which preferred information about both rewards and punishments, there were also neurons that significantly anticipated punishment information, and their proportion was much greater than expected by chance (Figure 3A, left; binomial test, $p < 10^{-8}$). However, these signals anticipating reward and punishment information appeared to be distributed independently across the neural population. That is, the reward and punishment information anticipation signals were not significantly correlated with each other (Figure 3A, left; rho = 0.074; p = 0.3705), and the number of individual neurons that anticipated both types of information (n = 10/149 (6.7%)) was not significantly greater than or less than what would be expected under the null hypothesis that these two forms of anticipation were independent of each other (STAR Methods; permutation test, p = 0.18). Of the ACC neurons that did anticipate both types of information, they were equally likely to anticipate them with the same sign (n = 5) or opposite signs (n = 5). Finally, in monkey 2, which did not prefer information about punishments, there was no significant neural anticipation of information about punishments (Figure 3B, left; n = 7/128, 5.5%) of task-responsive neurons; binomial test, p = 0.92). Thus, when comparing the two animals in terms of the proportion of their ACC neurons that anticipated information, the proportion was similar for reward information (Fisher's exact test, p = 0.34) but was significantly higher in monkey 1 than monkey 2 for punishment information (Fisher's exact test, p = 0.001).

These results show that ACC contains distinct neuronal processes suitable to mediate preferences for reward and punishment uncertainty resolution. We previously suggested that valence specificity in value processing in ACC could support flexible context-dependent choice behavior (Monosov, 2017). Similarly, the distinct processes reflected in single ACC neurons that anticipate reward and punishment information are well suited to support the individual differences in preferences that we observed in Figure 1C.

The vlPFC also contained substantial populations of task-responsive neurons that significantly anticipated either reward or punishment information (Figures 3A and 3B, right). However, the vlPFC displayed a very different pattern of results than ACC. First, in monkey 1, which preferred information about both rewards and punishments, vlPFC contained a notable subpopulation of neurons that significantly anticipated the resolution of both rewards and punishments (Figure 3A, right; n = 11/259, 4.25% of task-responsive neurons, significantly higher than the 0.25% of neurons expected by chance; binomial test, $p < 10^{-10}$). Indeed, signals anticipating reward and punishment information had a highly significant tendency to co-occur in the same neurons and to be coded in similar manners. Across all task-responsive neurons, the reward and punishment anticipation signals were significantly correlated with each other (Figure 3A, right; rho = 0.174; p = 0.0052), and there was a significant tendency for neurons to anticipate both reward and punishment information, compared with the null hypothesis that the two were independent (permutation test, p < 0.001). Notably, all of these vlPFC neurons anticipated both reward and punishment information by changing their activity in the same direction (Figure 3A, right; anticipatory activity taking the form of increases in activity, indicated by neurons in the upper right quadrant). Thus, there was a highly above chance proportion of neurons that anticipated both types of information with the same sign, compared with the null hypothesis that reward and punishment coding were independent of each other (permutation test, p < 0.001), and this was significantly greater than the proportion of neurons that anticipated reward and punishment information with opposite signs (permutation test, p < 0.001). These properties were in stark contrast with the same animal's ACC. Comparing the two areas, vlPFC had a significantly greater difference between the proportion of joint coding neurons and the proportion expected by chance under the null of independent coding (permutation test, p < 0.034), and this was specifically driven by neurons that anticipated reward and punishment information with the same sign (permutation test comparing proportions of joint coding neurons with the same sign, p < 0.001; analogous test for neurons with opposite signs, p = 0.11).

Monkey 2 also preferred information to resolve reward uncertainty but, unlike monkey 1, did not prefer information to resolve punishment uncertainty (Figure 1C). The vlPFC of monkey 2 reflected these behavioral biases. The vlPFC of monkey 2 contained many neurons anticipating information about rewards (Figure 3B, right; binomial test, $p < 10^{-10}$), but not information about punishment (n = 18/275 [6.6%] task-responsive neurons; not different from chance, binomial test, p = 0.30). Indeed, unlike monkey 1, there was no significant correlation between reward and punishment anticipation signals (Figure 3B, right; rho = 0.04; p = 0.4808), and there was no significant tendency for reward and punishment signals to occur in the same neurons (permutation test, p = 0.83) or to have the same sign (permutation test, p = 0.92). Thus, when comparing the two animals, monkey 1 had a significantly higher proportion of neurons that jointly anticipated reward and punishment information (permutation test, p < 0.001), and a significantly greater difference between the proportion of neurons that anticipated them with the same sign versus anticipated them with opposite signs (permutation test, p < 0.001). Taken together, these data show that ACC and vlPFC contain neural populations that anticipate information about uncertain rewards and punishments.

In addition, it suggests a possible relationship between information-anticipatory activity and behavioral information preferences. To visualize this, we plotted the prevalence of significant neuronal information-anticipatory activity as a function of the

uncertainty, and vlPFC had a substantial population that anticipated both with the same sign (green). Moreover, across the population, the reward and punishment information anticipation indexes were correlated. *p < 0.05, **p < 0.01, ***p < 0.001.

(B) Same plots for monkey 2. Unlike monkey 1, neither region had a significant number of neurons anticipating information to resolve punishment uncertainty or a significant correlation across valences.

(C) Summary of the relationship between choice preferences for information to resolve uncertainty (x axis; log odds from the analyses in Figure 1) and neural anticipation of information (y axis; % of neurons with significant information anticipation). Data are shown for each brain area, monkey, and valence. Error bars are bootstrap 68% CIs. Filled data points have significant neural information anticipation (p < 0.05, binomial test).

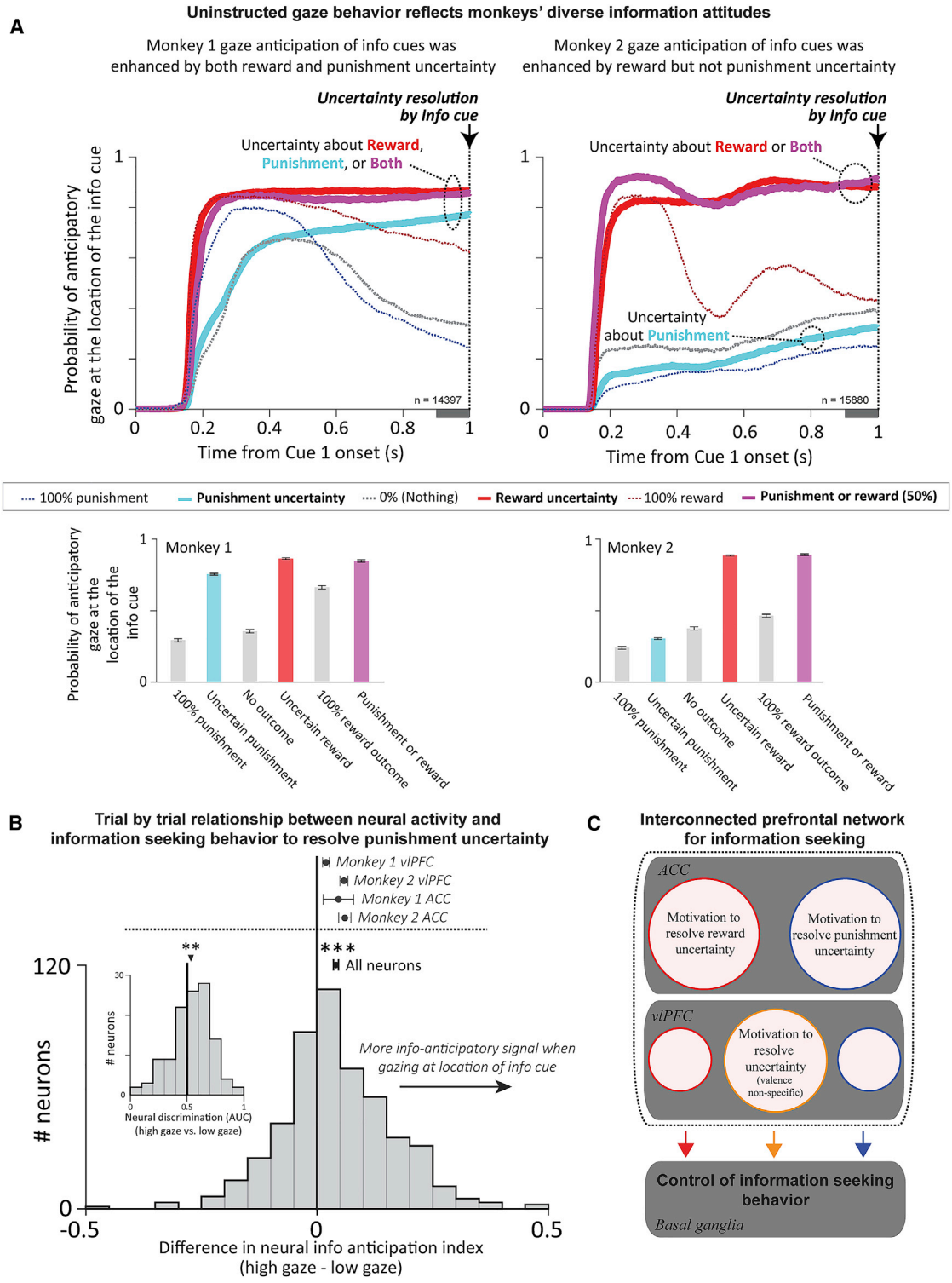

Figure 4. Single-trial relationship of neural activity to information-seeking behavior to resolve punishment uncertainty and summary of ACC-vlPFC circuit

(A) During Cue1 and subsequent cue presentations, monkeys were allowed to gaze freely; their gaze had no influence on the outcome. As shown previously (White et al., 2019), gaze during the informative block is attracted to the location of the upcoming informative cue before it appears to resolve reward uncertainty (top, thick red line). Crucially, anticipatory gaze also reflected attitudes to information to resolve punishment uncertainty. Monkey 1 (left) had prominent information-anticipatory gaze during punishment uncertainty (thick cyan line; summary in bar plots below). In contrast, monkey 2 (right) had prominent

(legend continued on next page)

behavioral preference to seek information to resolve uncertainty, for each of the 2 × 2 × 2 combinations of animals, areas, and outcome types (Figure 3C). The behavioral preference was quantified using the fitted weight of information × uncertainty from the behavioral logistic regression model (Figure 1C). In all six cases where animals expressed a preference for information to resolve uncertainty, ACC and vlPFC contained neurons that anticipated that type of information at significantly above chance levels. When, on average, an animal did not prefer information (monkey 2 for punishment information), both ACC and vlPFC had few neurons that anticipated that type of information, with a prevalence that was not significantly above chance. Hence the correlations among reward and punishment information anticipation signals in the vlPFC were not observed (Figures 3A and 3B, right). This suggests that the ACC-vlPFC network may be especially engaged when animals are motivated to seek information.

Trial-to-trial relationship between fluctuations in neuronal and behavioral information anticipation

To study the relationship of information seeking and neural activity on a trial-by-trial basis, we leveraged our recent finding that monkeys express a form of information-seeking behavior by anticipatorily gazing at objects that will provide informative visual cues to resolve reward uncertainty (Monosov, 2020; White et al., 2019). In the current data, we replicated those results, and in addition, we found that this information-anticipatory gaze mirrored the behavioral information preferences in our choice-task experiment (Figure 1C), consistent with a desire to resolve reward uncertainty. That is, in the realm of rewards, both monkeys had strong anticipatory gaze toward the location of upcoming informative cues and did so selectively when they were in a state of reward uncertainty (Figure 4A), persistently holding their gaze at the cue location until the cue appeared and their uncertainty was resolved.

We next asked whether the same relationship between information-seeking choice and gaze also held in the realm of punishments. Indeed, there was a clear correspondence between choice and anticipatory gaze: only monkey 1 had a choice preference for information to resolve punishment uncertainty, and only monkey 1 had selective anticipatory gaze toward informative cues to resolve punishment uncertainty (Figure 4A). Finally, we examined how reward and punishment uncertainty interacted to drive information-anticipatory gaze, using the bivalent 50% reward/50% punishment condition that presented both types of uncertainty at the same time. The results indicated that animals had strong information-anticipatory gaze as long as they preferred to resolve at least one of the two types of uncertainty. Notably, monkey 2 strongly anticipated information to resolve combined reward + punishment uncertainty despite not doing so for punishment uncertainty alone (Figure 4A, right). These data show that the monkeys' information-anticipatory gaze is a sensitive index of their motivation to seek information to resolve uncertainty.

With these findings in hand, we sought to relate the animal's motivation to seek information to information-anticipatory neural activity. In the realm of reward uncertainty, we previously showed that trial-to-trial fluctuations in ACC information-anticipatory activity predicted corresponding fluctuations in information-seeking gaze behavior (Monosov et al., 2020; White et al., 2019). Here, we asked whether a similar neural-behavioral link is true in the realm of punishment uncertainty; whether it extends to both ACC and vlPFC neurons; and whether this link occurs only in an animal with a net preference for this information (monkey 1) or also occurs in an animal that did not have a net preference for this information (monkey 2). To answer these questions, we took advantage of the fact that both monkeys had trial-to-trial variability in their anticipatory gaze for information to resolve punishment uncertainty, such that on some trials they gazed at the upcoming cue location and on other trials they did not (Figure 4A, "Uncertain punishment"). Hence for each neuron, we quantified how neural information anticipation was related to gaze by splitting each animal's data into "high gaze" and "low gaze" trials, calculating the neural punishment information anticipation index separately for each group of trials, and then taking the difference between the two indexes (STAR Methods). Thus, a positive difference between indexes indicates that neural punishment information-anticipatory signals were stronger on trials with more anticipatory gaze.

The results were clear: there were significantly stronger neural information-anticipatory signals on trials when animals had stronger behavioral measures of information seeking to resolve punishment uncertainty (Figure 4B). This effect was significant in each individual animal ($p < 0.001$ in each animal, signed-rank tests) and was significant or had a consistent trend in each individual combination of animal and area (Figure 4B, top; vlPFC: monkey 1, $p = 0.002$, monkey 2, $p < 0.001$; ACC: monkey 1, $p = 0.16$, monkey 2, $p < 0.001$, signed-rank tests). The effect tended to be somewhat stronger in monkey 2, perhaps because there was greater power to detect neural-behavioral relationships in that animal due to greater variation in behavior during punishment uncertainty (Figure 4A; monkey 1 is closer to ceiling, while monkey 2 had a more equal mix of "high gaze" and "low gaze" trials). Finally, we confirmed this finding by using ROC

information-anticipatory gaze only during reward uncertainty. In fact, monkey 2 had more anticipatory gaze on no-outcome trials (gray) than uncertain punishment trials ($p < 0.05$, signed-rank test). Error bars indicate SEM. Gray bar below the x axis is the analysis time window (100 ms before uncertainty resolution).
(B) Difference in each neuron's information anticipation index for uncertain punishments, when computed using trials with high versus low anticipatory gaze. Dot and error bars above histogram indicate mean and SEM pooling all neurons; asterisks indicate significant difference from 0 (***$p < 0.001$, signed-rank test). Mean and SEM for each area and each monkey are also shown. Pooled across areas, both monkeys had significant effects ($p < 0.001$). Monkey 2 had significantly stronger effects ($p < 0.01$, rank-sum test) consistent with the greater trial-to-trial variability this monkey displayed in gaze behavior (A). Pooled across monkeys, both areas had significant effects ($p < 0.001$) with no difference between areas ($p = 0.22$, rank-sum test). Inset: neural firing rate discrimination between punishment uncertainty trials that had high versus low anticipatory gaze, based on separate calculations for each punishment condition (see STAR Methods).
(C) Summary of the ACC-vlPFC circuit coding for information seeking to resolve reward and punishment uncertainty. Anatomical and functional connections with the basal ganglia are based on our previous work showing that the basal ganglia, in particular the internal capsule bordering dorsal striatum (White et al., 2019), controls gaze shifts to seek advance information about uncertain rewards. Size of circles do not denote % of neurons within each region.

analysis to directly compare neural firing rates between "high gaze" versus "low gaze" trials, while controlling for any potential differences in neural activity or behavior across the different punishment probability conditions (STAR Methods). This analysis revealed significantly higher neural activity on trials when monkeys expressed high motivation to reduce punishment uncertainty (Figure 4B, inset).

Importantly, although enhanced information-anticipatory activity was linked to enhanced information-anticipatory behavior, information-anticipatory activity was not simply the result of neurons encoding specific behavioral responses, such as licking, blinking, or gazing at the cue. First, consistent with previous research, these behaviors were all strongly influenced by the probability of reward or punishment (Figures 4 and S1), while information-anticipatory activity was primarily driven by uncertainty (Figures 2, 3, and S6). Second, the time courses of licking and blinking were distinct from the time course of information-anticipatory activity (Figures S1 and S7). Finally, information-anticipatory activity was still highly significant after controlling for gaze state (STAR Methods). Thus, the link between neurons and behavior was consistent with a motivational signal rather than a sensory or motor signal.

DISCUSSION

We performed the first neuronal investigation of informational preferences to resolve uncertainty about future rewards and punishments. We found that informational attitudes about rewards and punishments are dissociable at both the behavioral and neuronal levels. This result mirrors important observations in human behavior: although most people prefer to resolve their uncertainty about future rewards, they display considerable variability in preferences for information about punishments or other undesirable outcomes (Charpentier et al., 2018; Miller, 1987, 1995; Niehoff and Oosterwijk, 2020; Oosterwijk, 2017).

We identified an ACC-vlPFC network containing neurons that selectively encode opportunities to gain information to resolve uncertainty. Furthermore, their neural code was closely linked to informational preferences, both in terms of individual differences in decision making and trial-to-trial fluctuations in information-seeking behavior. This information-anticipatory activity was not simply due to neurons encoding behavioral responses.

Within this network we found a key difference between ACC and vlPFC. Although both regions contained neurons that anticipated information to resolve uncertainty, the ACC contained largely independent activations for each specific valence, such as anticipating information about punishments but not rewards or vice versa. These results are consistent with our and others' previous work indicating that ACC supports behavioral control flexibly in a valence-specific manner; that is, ACC neurons can signal decision and learning related variables in relation to either future rewards or future punishments (Monosov, 2017; Monosov et al., 2020). By contrast, the vlPFC also had a significant subpopulation of neurons that anticipated information in a bivalent manner, with similar neural codes for resolving uncertainty about both punishments and rewards (Figures 2 and 4C).

We found differences among monkeys in the neural signatures of the motivation to resolve punishment uncertainty that reflected differences in their behavioral attitudes (Figure 1C). Importantly, these differences were likely not due to differences in recording locations. We used imaging and functional electrophysiological mapping to find the same regions in the ACC that were preferentially enriched with neurons that anticipated reward uncertainty resolution. These areas matched our previous data (White et al., 2019). At these sites, in ACC, we found that punishment and reward uncertainty resolution-anticipating neurons were highly intermingled; there were no apparent anatomical differences in their locations (also see Monosov, 2017). This fits well with previous reports showing that positive and negative value neurons and valence-specific neurons are not anatomically separable within area 24, which was the subject of this study (Hosokawa et al., 2013; Kennerley et al., 2009, 2011; Monosov, 2017; Monosov et al., 2020; Wallis and Kennerley, 2010). In turn, vlPFC recordings were verified by imaging and aimed directly at the location of dense ACC projections (Figure 1).

In addition, these differences were not due to differences across the two animals in training or understanding the task. In fact, the monkeys had remarkably similar attitudes toward most attributes of the stimuli, including reward probability, punishment probability, reward uncertainty, punishment uncertainty, and the main effect of information. Furthermore, neural activity in the ACC-vlPFC network strongly reflected both monkeys' desire to resolve reward uncertainty. The key difference was that monkey 1 sought information to resolve punishment uncertainty, and monkey 2 did not; this was also differentiated by neural representations in ACC and vlPFC. One other difference among the monkeys that warrants consideration was that the effect of punishment probability on choice was relatively smaller in monkey 2 than in monkey 1. Humans show variability in information attitude across many distinct contexts, particularly about the resolution of uncertainty about punishments. It is therefore possible that changing the subjective aversiveness of punishments could impact the individual differences we observe. If so, we would predict that these changes would also be reflected in the ACC-vlPFC network. In fact, this conjecture is supported by the results of Figure 4. Both monkeys had variability in their trial-by-trial information attitudes that were linked to concomitant changes in ACC-vlPFC network activity. Hence in both animals, the activity in this network was related to trial-by-trial information attitudes.

An important question is how much ACC-vlPFC activity anticipates opportunities to obtain information per se, versus anticipates the subjective value of that information. Our data do not conclusively resolve this, but several lines of evidence are consistent with the latter: (1) information signals and information preferences were both strongest for uncertain outcomes (Figure S6); (2) information signals were only significant when information was preferred; (3) vlPFC neurons significantly anticipated reward and punishment information with the same sign only when both types of information were preferred; and (4) punishment information signals were linked to trial-to-trial fluctuations in information-anticipatory behavior, which in turn matched behavioral preferences.

To date, little is known about single neurons' activity in the vlPFC areas we recorded, particularly anterior-ventral 47/12o. This region is anterior-ventral to the auditory domain within

vlPFC (Romanski and Goldman-Rakic, 2002). Also, to our knowledge, it is lateral (and in some cases ventral) to regions studied in previous electrophysiological experiments in lateral orbitofrontal recordings in monkeys, which concentrated most prominently on area 13 (Blanchard et al., 2015; Cai and Padoa-Schioppa, 2012; Hosokawa et al., 2013; Kennerley et al., 2011; Kennerley and Wallis, 2009; Luk and Wallis, 2013; Padoa-Schioppa and Cai, 2011; Rich and Wallis, 2014). A recent study lesioned vlPFC in monkeys and found deficits in trials in which the animals were required to track reward probability to assess how available or not available reward might be (Murray and Rudebeck, 2018; Rudebeck et al., 2017). Another study showed that the lateral regions of the orbital bank somewhat overlapping with our region of interest derive their trial-to-trial value information from external stimuli relatively more so than from internal representations (Rich and Wallis, 2014). Our work adds to these previous findings by showing that many single neurons in vlPFC regions 47/12o have distinct signals that encode opportunities to gain advance information about future uncertain outcomes, which in our study indeed is obtained from external visual cues. Notably, this information-related activity we observed was not related to the animal's overall preference for a particular stimulus or to its expected reward value; instead, this activity was specifically related to the animals' preference to gain information to resolve uncertainty about both rewards and punishments.

These data are related to a line of work that suggests that vlPFC is involved widely in surprise processing (Grohn et al., 2020) and participates in credit assignment in probabilistic and dynamic settings (Noonan et al., 2011, 2017). Our data suggest that these processes may be supported by information-seeking-related functions of vlPFC neurons. For example, one can interpret their bivalent information-anticipatory activity as anticipating the moment of surprise (or of absolute reward prediction error) when uncertainty will be resolved and the trial's outcome will be revealed. This would permit vlPFC to highlight the key moments in a task when cognitive processes must be recruited to interpret new feedback, perform credit assignment, and promote learning and adjustments in behavior.

Here and in our previous work (White et al., 2019), similar overlapping populations of neurons anticipated the resolution of reward uncertainty by both (1) informative visual cues and (2) the delivery (or omission) of the uncertain reward outcomes themselves (Figure S7). Interestingly, our data suggest that distinct populations of neurons perform these functions for aversive/noxious punishments: one population anticipates informative cues, while a second tonically signals the level of uncertainty leading up to uncertain punishment outcomes (Figures S7 and S8). Future studies must resolve how these distinct populations support behavior related to punishment uncertainty.

Of the diverse theoretical mechanisms that have been proposed to motivate non-instrumental information seeking, many can be divided into two types: explicit motivation to resolve uncertainty and overweighting of desirable versus undesirable information (Bromberg-Martin and Monosov, 2020). Our data show that the ACC-vlPFC network is highly suitable for the former type of mechanism. The latter type of mechanism could be implemented by distinct or overlapping brain networks (e.g., Iigaya et al., 2020) because multiple mechanisms may operate in parallel to motivate information seeking (Bromberg-Martin and Monosov, 2020; Kobayashi et al., 2019; Sharot and Sunstein, 2020). We believe that the emerging field of research on information seeking will shed further light on the distinct circuits and motivational mechanisms that govern these informational preferences.

STAR★METHODS

Detailed methods are provided in the online version of this paper and include the following:

- KEY RESOURCES TABLE
- RESOURCE AVAILABILITY
  - Lead contact
  - Materials availability
  - Data and code availability
- EXPERIMENTAL MODEL AND SUBJECT DETAILS
- METHOD DETAILS
  - Data acquisition
  - Chemical tracer injections
  - Manganese enhanced magnetic resonance imaging tracing
  - Behavioral tasks
- QUANTIFICATION AND STATISTICAL ANALYSIS
  - Analysis of behavioral choice
  - Analysis of neural coding prevalence in each neural population
  - Trial-by-trial relationship of activity and Info Anticipation
  - Analysis of neural activity as a function of gaze state

SUPPLEMENTAL INFORMATION

Supplemental information can be found online at https://doi.org/10.1016/j.neuron.2021.05.013.

ACKNOWLEDGMENTS

This work was supported by the National Institute of Mental Health under award numbers R01MH110594 and R01MH116937 (to I.E.M.), by the McKnight Foundation award (to I.E.M.), and by R01MH106435 and R01MH045573 to (S.N.H.). We are grateful to Kim Kocher for great animal care and animal training. We also thank Dr. Lawrence Snyder and Jonathon Tucker for assistance with imaging experiments and Dr. Joel Price for allowing us to digitize his anatomical collection and to utilize some of it in this manuscript.

AUTHOR CONTRIBUTIONS

A.J. and I.E.M. performed the experiments. All authors analyzed the data and wrote the manuscript. I.E.M. guided the research.

DECLARATION OF INTERESTS

The authors declare no competing interests.

Received: February 10, 2021
Revised: March 30, 2021
Accepted: May 10, 2021
Published: June 11, 2021

REFERENCES

An, X., Bandler, R., Ongür, D., and Price, J.L. (1998). Prefrontal cortical projections to longitudinal columns in the midbrain periaqueductal gray in macaque monkeys. J. Comp. Neurol. *401*, 455–479.

Badia, P., Harsh, J., and Abbott, B. (1979). Choosing between predictable and unpredictable shock conditions: Data and theory. Psychol. Bull. *86*, 1107–1131.

Barberini, C.L., Morrison, S.E., Saez, A., Lau, B., and Salzman, C.D. (2012). Complexity and competition in appetitive and aversive neural circuits. Front. Neurosci. *6*, 170.

Blanchard, T.C., Hayden, B.Y., and Bromberg-Martin, E.S. (2015). Orbitofrontal cortex uses distinct codes for different choice attributes in decisions motivated by curiosity. Neuron *85*, 602–614.

Bromberg-Martin, E.S., and Hikosaka, O. (2009). Midbrain dopamine neurons signal preference for advance information about upcoming rewards. Neuron *63*, 119–126.

Bromberg-Martin, E.S., and Monosov, I.E. (2020). Neural circuitry of information seeking. Curr. Opin. Behav. Sci. *35*, 62–70.

Cai, X., and Padoa-Schioppa, C. (2012). Neuronal encoding of subjective value in dorsal and ventral anterior cingulate cortex. J. Neurosci. *32*, 3791–3808.

Charpentier, C.J., Bromberg-Martin, E.S., and Sharot, T. (2018). Valuation of knowledge and ignorance in mesolimbic reward circuitry. Proc. Natl. Acad. Sci. USA *115*, E7255–E7264.

Christopoulos, G.I., Tobler, P.N., Bossaerts, P., Dolan, R.J., and Schultz, W. (2009). Neural correlates of value, risk, and risk aversion contributing to decision making under risk. J. Neurosci. *29*, 12574–12583.

Cox, R.W. (1996). AFNI: software for analysis and visualization of functional magnetic resonance neuroimages. Comput. Biomed. Res. *29*, 162–173.

Daddaoua, N., Lopes, M., and Gottlieb, J. (2016). Intrinsically motivated oculomotor exploration guided by uncertainty reduction and conditioned reinforcement in non-human primates. Sci. Rep. *6*, 20202.

Daye, P.M., Monosov, I.E., Hikosaka, O., Leopold, D.A., and Optican, L.M. (2013). pyElectrode: an open-source tool using structural MRI for electrode positioning and neuron mapping. J. Neurosci. Methods *213*, 123–131.

Eliaz, K., and Schotter, A. (2007). Experimental testing of intrinsic preferences for noninstrumental information. Am Econ Rev *97*, 166–169.

Eschenko, O., Canals, S., Simanova, I., and Logothetis, N.K. (2010). Behavioral, electrophysiological and histopathological consequences of systemic manganese administration in MEMRI. Magn. Reson. Imaging *28*, 1165–1174.

Fanselow, M.S. (1979). Naloxone attenuates rat's preference for signaled shock. Physiol. Psychol. *7*, 70–74.

Ferry, A.T., Ongür, D., An, X., and Price, J.L. (2000). Prefrontal cortical projections to the striatum in macaque monkeys: evidence for an organization related to prefrontal networks. J. Comp. Neurol. *425*, 447–470.

Gottlieb, J., Oudeyer, P.-Y., Lopes, M., and Baranes, A. (2013). Information-seeking, curiosity, and attention: computational and neural mechanisms. Trends Cogn. Sci. *17*, 585–593.

Gottlieb, J., Cohanpour, M., Li, Y., Singletary, N., and Zabeh, E. (2020). Curiosity, information demand and attentional priority. Curr. Opin. Behav. Sci. *35*, 83–91.

Grohn, J., Schüffelgen, U., Neubert, F.-X., Bongioanni, A., Verhagen, L., Sallet, J., Kolling, N., and Rushworth, M.F.S. (2020). Multiple systems in macaques for tracking prediction errors and other types of surprise. PLoS Biol. *18*, e3000899.

Hosokawa, T., Kennerley, S.W., Sloan, J., and Wallis, J.D. (2013). Single-neuron mechanisms underlying cost-benefit analysis in frontal cortex. J. Neurosci. *33*, 17385–17397.

Hsu, D.T., and Price, J.L. (2007). Midline and intralaminar thalamic connections with the orbital and medial prefrontal networks in macaque monkeys. J. Comp. Neurol. *504*, 89–111.

Hsu, D.T., and Price, J.L. (2009). Paraventricular thalamic nucleus: subcortical connections and innervation by serotonin, orexin, and corticotropin-releasing hormone in macaque monkeys. J. Comp. Neurol. *512*, 825–848.

Hunt, L.T., Malalasekera, W.M.N., de Berker, A.O., Miranda, B., Farmer, S.F., Behrens, T.E.J., and Kennerley, S.W. (2018). Triple dissociation of attention and decision computations across prefrontal cortex. Nat. Neurosci. *21*, 1471–1481.

Iigaya, K., Hauser, T.U., Kurth-Nelson, Z., O'Doherty, J.P., Dayan, P., and Dolan, R.J. (2020). The value of what's to come: Neural mechanisms coupling prediction error and the utility of anticipation. Sci. Adv. *6*, eaba3828.

Kennerley, S.W., and Wallis, J.D. (2009). Evaluating choices by single neurons in the frontal lobe: outcome value encoded across multiple decision variables. Eur. J. Neurosci. *29*, 2061–2073.

Kennerley, S.W., Dahmubed, A.F., Lara, A.H., and Wallis, J.D. (2009). Neurons in the frontal lobe encode the value of multiple decision variables. J. Cogn. Neurosci. *21*, 1162–1178.

Kennerley, S.W., Behrens, T.E., and Wallis, J.D. (2011). Double dissociation of value computations in orbitofrontal and anterior cingulate neurons. Nat. Neurosci. *14*, 1581–1589.

Kobayashi, K., Ravaioli, S., Baranès, A., Woodford, M., and Gottlieb, J. (2019). Diverse motives for human curiosity. Nat. Hum. Behav. *3*, 587–595.

Ledbetter, N.M., Chen, C.D., and Monosov, I.E. (2016). Multiple Mechanisms for Processing Reward Uncertainty in the Primate Basal Forebrain. J. Neurosci. *36*, 7852–7864.

Lerman, C., Hughes, C., Lemon, S.J., Main, D., Snyder, C., Durham, C., Narod, S., and Lynch, H.T. (1998). What you don't know can hurt you: adverse psychologic effects in members of BRCA1-linked and BRCA2-linked families who decline genetic testing. J. Clin. Oncol. *16*, 1650–1654.

Luk, C.H., and Wallis, J.D. (2013). Choice coding in frontal cortex during stimulus-guided or action-guided decision-making. J. Neurosci. *33*, 1864–1871.

McCoy, A.N., and Platt, M.L. (2005). Risk-sensitive neurons in macaque posterior cingulate cortex. Nat Neurosci *8* (9), 1220–1227. https://doi.org/10.1038/nn1523.

Miller, S.M. (1987). Monitoring and blunting: validation of a questionnaire to assess styles of information seeking under threat. J. Pers. Soc. Psychol. *52*, 345–353.

Miller, S.M. (1995). Monitoring versus blunting styles of coping with cancer influence the information patients want and need about their disease. Implications for cancer screening and management. Cancer *76*, 167–177.

Miller, R.R., Greco, C., Vigorito, M., and Marlin, N.A. (1983). Signaled tailshock is perceived as similar to a stronger unsignaled tailshock: implications for a functional analysis of classical conditioning. J. Exp. Psychol. Anim. Behav. Process. *9*, 105–131.

Monosov, I.E. (2017). Anterior cingulate is a source of valence-specific information about value and uncertainty. Nat. Commun. *8*, 134.

Monosov, I.E. (2020). How Outcome Uncertainty Mediates Attention, Learning, and Decision-Making. Trends Neurosci. *43*, 795–809.

Monosov, I.E., and Hikosaka, O. (2013). Selective and graded coding of reward uncertainty by neurons in the primate anterodorsal septal region. Nat. Neurosci. *16*, 756–762.

Monosov, I.E., Trageser, J.C., and Thompson, K.G. (2008). Measurements of simultaneously recorded spiking activity and local field potentials suggest that spatial selection emerges in the frontal eye field. Neuron *57*, 614–625.

Monosov, I.E., Leopold, D.A., and Hikosaka, O. (2015). Neurons in the Primate Medial Basal Forebrain Signal Combined Information about Reward Uncertainty, Value, and Punishment Anticipation. J. Neurosci. *35*, 7443–7459.

Monosov, I.E., Haber, S.N., Leuthardt, E.C., and Jezzini, A. (2020). Anterior Cingulate Cortex and the Control of Dynamic Behavior in Primates. Curr. Biol. *30*, R1442–R1454.

Murayama, Y., Weber, B., Saleem, K.S., Augath, M., and Logothetis, N.K. (2006). Tracing neural circuits in vivo with Mn-enhanced MRI. Magn. Reson. Imaging *24*, 349–358.

Murray, E.A., and Rudebeck, P.H. (2018). Specializations for reward-guided decision-making in the primate ventral prefrontal cortex. Nat. Rev. Neurosci. *19*, 404–417.

Niehoff, E., and Oosterwijk, S. (2020). To know, to feel, to share? Exploring the motives that drive curiosity for negative content. Curr. Opin. Behav. Sci. *35*, 56–61.

Noonan, M.P., Mars, R.B., and Rushworth, M.F. (2011). Distinct roles of three frontal cortical areas in reward-guided behavior. J. Neurosci. *31*, 14399–14412.

Noonan, M.P., Chau, B.K.H., Rushworth, M.F.S., and Fellows, L.K. (2017). Contrasting effects of medial and lateral orbitofrontal cortex lesions on credit assignment and decision-making in humans. J. Neurosci. *37*, 7023–7035.

Ongür, D., and Price, J.L. (2000). The organization of networks within the orbital and medial prefrontal cortex of rats, monkeys and humans. Cereb. Cortex *10*, 206–219.

Oosterwijk, S. (2017). Choosing the negative: A behavioral demonstration of morbid curiosity. PLoS ONE *12*, e0178399.

Oosterwijk, S., Snoek, L., Tekoppele, J., Engelbert, L.H., and Scholte, H.S. (2020). Choosing to view morbid information involves reward circuitry. Sci. Rep. *10*, 15291.

Padoa-Schioppa, C., and Cai, X. (2011). The orbitofrontal cortex and the computation of subjective value: consolidated concepts and new perspectives. Ann. N Y Acad. Sci. *1239*, 130–137.

Pautler, S.E., Vallely, J.F., and Denstedt, J.D. (1998). Perinephric abscess following extracorporeal shockwave lithotripsy. Can. J. Urol. *5*, 623–626.

Rich, E.L., and Wallis, J.D. (2014). Medial-lateral organization of the orbitofrontal cortex. J. Cogn. Neurosci. *26*, 1347–1362.

Romanski, L.M., and Goldman-Rakic, P.S. (2002). An auditory domain in primate prefrontal cortex. Nat. Neurosci. *5*, 15–16.

Rudebeck, P.H., Saunders, R.C., Lundgren, D.A., and Murray, E.A. (2017). Specialized representations of value in the orbital and ventrolateral prefrontal cortex: desirability versus availability of outcomes. Neuron *95*, 1208–1220.e5.

Saleem, K.S., Pauls, J.M., Augath, M., Trinath, T., Prause, B.A., Hashikawa, T., and Logothetis, N.K. (2002). Magnetic resonance imaging of neuronal connections in the macaque monkey. Neuron *34*, 685–700.

Sharot, T., and Sunstein, C.R. (2020). How people decide what they want to know. Nat. Hum. Behav. *4*, 14–19.

Simmons, J.M., Saad, Z.S., Lizak, M.J., Ortiz, M., Koretsky, A.P., and Richmond, B.J. (2008). Mapping prefrontal circuits in vivo with manganese-enhanced magnetic resonance imaging in monkeys. J. Neurosci. *28*, 7637–7647.

So, N.Y., and Stuphorn, V. (2010). Supplementary eye field encodes option and action value for saccades with variable reward. J. Neurophysiol. *104*, 2634–2653.

Stewart, N., Hermens, F., and Matthews, W.J. (2016). Eye movements in risky choice. J. Behav. Decis. Making *29*, 116–136.

Sutton, R.S., and Barto, A.G. (1998). Reinforcement Learning: An Introduction, Vol 1 (MIT Press).

Taghizadeh, B., Foley, N.C., Karimimehr, S., Cohanpour, M., Semework, M., Sheth, S.A., Lashgari, R., and Gottlieb, J. (2020). Reward uncertainty asymmetrically affects information transmission within the monkey fronto-parietal network. Commun. Biol. *3*, 594.

Tsuda, A., Ida, Y., Satoh, H., Tsujimaru, S., and Tanaka, M. (1989). Stressor predictability and rat brain noradrenaline metabolism. Pharmacol. Biochem. Behav. *32*, 569–572.

Wallis, J.D., and Kennerley, S.W. (2010). Heterogeneous reward signals in prefrontal cortex. Curr. Opin. Neurobiol. *20*, 191–198.

White, J.K., and Monosov, I.E. (2016). Neurons in the primate dorsal striatum signal the uncertainty of object-reward associations. Nat. Commun. *7*, 12735.

White, J.K., Bromberg-Martin, E.S., Heilbronner, S.R., Zhang, K., Pai, J., Haber, S.N., and Monosov, I.E. (2019). A neural network for information seeking. Nat. Commun. *10*, 5168.

STAR★METHODS

KEY RESOURCES TABLE

REAGENT or RESOURCE	SOURCE	IDENTIFIER
Experimental models: Organisms/strains		
Rhesus Macaques	PrimGen	Macaca mulatta
	NIH Animal Center at Poolesville	N/A
Software and algorithms		
MATLAB	Mathworks	https://www.mathworks.com/

RESOURCE AVAILABILITY

Lead contact

Further information and requests for resources, data, and code should be directed to the Lead Contact, Dr. Ilya E. Monosov (ilya.monosov@gmail.com).

Materials availability

This study did not generate new unique reagents

Data and code availability

Original source data are available upon reasonable request from the Lead Contact.

EXPERIMENTAL MODEL AND SUBJECT DETAILS

Two adult male monkeys (*Macaca mulatta*; Monkey M1 and Monkey M2; ages: 7-10 years old) were used for recording and imaging experiments. All these procedures conform to the Guide for the Care and Use of Laboratory Animals and were approved by the Institutional Animal Care and Use Committee at Washington University. Anatomical tracer experiments were carried out on separate animals from those used for electrophysiology. Two adult male monkeys (*Macaca mulatta*) were used for these experiments. Procedures were conducted in accordance with the Institute of Laboratory Animal Resources Guide for the Care and Use of Laboratory Animals and approved by the University Committee on Animal Resources at the University of Rochester and by Washington University Institutional Animal Care and Use Committee.

METHOD DETAILS

A plastic head holder and plastic recording chamber were fixed to the skull under general anesthesia and sterile surgical conditions. For ACC, the chambers were tilted laterally by 35° and aimed at the anterior cingulate and the anterior regions of the basal ganglia. After the monkeys recovered from surgery, they participated in the behavioral and neurophysiological experiments. For vlPFC, novel grids were manufactured to approach vlPFC at an extreme lateral angle (up to 20 degrees) such that electrodes can be accurately targeted to the sites of strongest anatomical connectivity with the ACC.

Data acquisition

While the monkeys participated in the behavioral procedure, we recorded single neurons in the anterior cingulate and the ventral lateral prefrontal cortex, areas 47/12o. The recording sites were determined with 1 mm-spacing grid system and with the aid of MR (3T) and CT images. This imaging-based estimation of neuron recording locations was aided by custom-built software (PyElectrode, Daye et al., 2013). Single-unit recording was performed using glass-coated electrodes (Alpha Omega) and 16 channel linear arrays (v-probes, Plexon). These devices were inserted into the brain through a stainless-steel guide tube and advanced by an oil-driven micromanipulator (MO-97A, Narishige).

Signal acquisition (including amplification and filtering) was performed using a Plexon 40 kHZ recording system. Action potential waveforms were identified online by multiple time-amplitude windows, and the isolation was refined offline (Plexon Offline Sorter) clustering by the first three principal components and non-linear energy.

Because in Monkey 1 (M1), we use electrophysiological identification of information-anticipating neurons to perform in-vivo tracing (MEMRI), we functionally mapped M1 ACC using single unit (single channel) electrophysiology, the most precise method that we used in the past to target anatomical injections (Monosov et al., 2015). In M1, as previously, we recorded only neurons that were judged online to be task responsive, that is exhibiting inhibition or excitation to any task Cue1 (Monosov, 2017; White et al., 2019; White and Monosov, 2016). This rendered 162 neurons, of which 149 were task responsive (Kruskal-Wallis test across all PS epochs, $p < 0.01$). For Monkey 2 (M2), we used linear arrays and included any well-isolated neuron, yielding 128/334 neurons that were task responsive (38%). This matched our previous measurements in M1 (White et al., 2019). Next, after we carefully targeted the tracer in M1 using single unit electrophysiology to identify vlPFC regions receiving ACC inputs, and confirmed MEMRI accuracy using chemical tracing, we recorded in vlPFC using linear arrays and confirmed accuracy using imaging in both monkeys. In M1, this yielded 259/711 task responsive neurons and 275/452 neurons in M2.

ACC recordings were performed in the range of ~8-15 mm anterior (mean: ~12 mm) in M1 and ~7-14 mm anterior (mean: ~11 mm) in M2 relative to the center of the anterior commissure (AC; located ~21 mm anterior to the interaural 0). The medial-lateral extent of ACC recording spanned the lateral bank of the ACC matching our previous studies (Monosov, 2017; White et al., 2019). vlPFC recordings were performed ~14mm from the center of the AC in M1, and in the range of ~8-14mm anterior (mean: ~11 mm) in M2 relative to the center of the AC. The medial-lateral extent of vlPFC recording was from ~1 mm medial-2 mm lateral relative to the location of the electrode in Figure 1D. Recording locations were verified by MRI and CT imaging (Daye et al., 2013).

Eye position was obtained with an infrared video camera (Eyelink, SR Research). Behavioral events and visual stimuli were controlled by MATLAB (Mathworks, Natick, MA) with Psychophysics Toolbox extensions. Juice, used as reward, was delivered with a solenoid delivery reward system (CRIST Instruments). Juice-related licking was measured and quantified using previously described methods (Ledbetter et al., 2016; Monosov, 2017; Monosov and Hikosaka, 2013; White et al., 2019). Airpuff (~35 psi) was delivered through a narrow tube placed ~6–8 cm from the monkey's face (Monosov, 2017).

Chemical tracer injections

For retrograde tracing experiments (Figure 1D; Figure S4), two adult male macaque monkeys were used (*Macaca mulatta*). The monkey received ketamine 10 mg/kg, diazepam 0.25 mg/kg, and atropine 0.04 mg/kg IM in the cage. A surgical plane of anesthesia was maintained via 1%–3% isoflurane in 100% oxygen via vaporizer. Temperature, heart rate, and respiration were monitored throughout the surgery. The monkey was placed in a Kopf stereotaxic, a midline scalp incision was made, and the muscle and fascia were displaced laterally to expose the skull. A craniotomy (~2–3 cm^2) was made over the region of interest, and small dural incisions were made only at injection sites. The monkey received an injection of Lucifer Yellow (LY) tracer (40 nl, 10% in 0.1 M phosphate buffer (PB), pH 7.4; Invitrogen).

The tracer was pressure-injected over 10 min using a 0.5 μL Hamilton syringe. Following each injection, the syringe remained *in situ* for 20–30 min. Twelve to 14 days after surgery, the monkey was again deeply anesthetized and perfused with saline followed by a 4% paraformaldehyde/1.5% sucrose solution in 0.1 M PB, pH 7.4. The brain was postfixed overnight, and cryoprotected in increasing gradients of sucrose (10, 20, and 30%). Serial sections of 50 μm were cut on a freezing microtome into 0.1 M PB or cryoprotectant solution. One in eight sections was processed free-floating for immunocytochemistry to visualize the tracers. Tissue was incubated in primary anti-LY (1:3000 dilution; Invitrogen) in 10% NGS and 0.3% Triton X-100 (Sigma-Aldrich) in PB for four nights at 4 °C. Following extensive rinsing, the tissue was incubated for 40 min in biotinylated secondary anti-rabbit antibody made in goat (1:200; Vector BA-1000) followed by incubation with the avidin–biotin complex solution (Vectastain ABC kit, Vector Laboratories). Immunoreactivity was visualized using standard DAB procedures. Staining was intensified by incubating the tissue for 5–15 s in a solution of 0.05% 3,3′-diaminobenzidine tetra-hydrochloride, 0.025% cobalt chloride, 0.02% nickel ammonium sulfate, and 0.01% H_2O_2. Sections were mounted onto gel-coated slides, dehydrated, defatted in xylene, and coverslipped with Permount. Retrogradely labeled input cells were identified under brightfield microscopy (x20). StereoInvestigator software (Micro-BrightField) was used to stereologically count labeled cells with an even sampling (1.2 mm of interval between slides).

Anterograde cases in the Supplemental Materials come from the newly-digitized collection of anatomical tracers from the laboratories of Dr. Joel Price. For those injections, BDA (10,000 kDA) was used as anterograde tracer and processed as described previously (An et al., 1998; Ferry et al., 2000; Hsu and Price, 2007, 2009; Ongür and Price, 2000).

Manganese enhanced magnetic resonance imaging tracing

To localize where the ACC information anticipation-related functional hotspot most strongly projects, we used manganese-enhanced MRI tracing (MEMRI). The method relies on two properties of manganese ions: (1) the manganese ion (Mn^{2+}) is a calcium ion analog and is therefore taken up by neurons and transported in an anterograde fashion; and (2) Mn^{2+} increases the MR intensity of voxels (Pautler et al., 1998; Saleem et al., 2002; Simmons et al., 2008). Therefore, by injecting Mn^{2+} directly into the brain, we can trace neuronal pathways using standard T1-weighted MRI. To choose the injection site, we recorded neuronal activity in the ACC before the injection and verified that the information anticipation neurons were there and used T1 MRI to double check that this location roughly matched the region we previously quantitatively identified as enriched in information anticipation related neurons (White et al., 2019). We then used a small metal cannula to target the injection to the appropriate depth of high concentration of information anticipation-related neurons. We injected 0.15 μL of 150 mM solution of manganese chloride. This concentration was previously shown to be nontoxic (Eschenko et al., 2010; Simmons et al., 2008). The injection was made over an approximately 30-minute

duration. We then waited approximately 15 minutes to retract the cannula. We first retracted 0.5 mm and waited for approximately 10 minutes, and then retracted completely and prepared the monkey for MRI.

MR anatomical images were acquired in a 3T horizontal scanner. The monkey's head was placed in the scanner in stereotactic position. To minimize changes in RF across scans, as previously (Monosov et al., 2015), we made sure that the MR surface coil was always in roughly the same location (relative to the monkey's head) before acquiring a 3D volume with an 0.5 mm isotropic voxel size. Each 3D volume took ~15 min to acquire without averaging. Five baseline pre-injection scans were collected a week before the injection day. On the injection day, a single T1 scan was collected ~1 h after the injection was finished to visualize Mn^{2+}. Five post-injection scans were collected 24 hours after the injection. Because in our previous studies we found that MN++ accumulates in subcortical structures over time (unpublished), we also scanned 96 hours after the injection to further validate our methods and this observation (data available upon request). All scans were obtained using the same acquisition under isoflurane gas anesthesia.

As in previous monkey MEMRI experiments, we could not detect manganese transport by eye 24 h after the injection (Simmons et al., 2008). To visualize the transport, we calculated the percentage increase of voxel intensity after the injection by comparing averaged pre-injection scan with averaged post-injection scans. This was the same procedure and analyses that we developed with the Leopold laboratory (Monosov et al., 2015). Before doing this, the averaged MRIs were processed by the Analysis of Functional NeuroImages (AFNI) toolkit (Cox, 1996). First, the image nonuniformity was reduced (AFNI function: 3dUniformize). Second, the images were resampled, doubling the number of voxels (AFNI function: 3dresample). Third, the post-injection scans were aligned with the average pre-injection baseline scan using affine transforms (AFNI function: 3dAllineate). Fifth, the averaged images (pre and post) were smoothed with a 3D Gaussian filter (σ = 0.2 mm). Last, before calculating the percentage increase, each average scan was normalized by dividing by the average intensity value of 5 mm^3 of cortex (Monosov et al., 2015).

Behavioral tasks

The information task used in this study is as displayed in Figure 1A. The task began with the appearance of a small circular trial start cue at the center of the screen. This trial start cue then disappeared and was followed in succession by a donut shaped visual fractal Cue1 (~4° radius) that was displayed for a fixed duration (1 second). Then, within it, a square shaped fractal Cue2 appeared, filling the blank space within it. Then, in 1.5 s the donut shaped Cue1 disappeared, indicating that in 0.75 s the trial's scheduled outcome would occur. Then, the screen went blank and simultaneously the outcome was delivered.

The stimuli were presented randomly on either the left or right side of the screen (~12.5°). The Cue1s came in two types. The information-predictive Cue1s predicted juice reward (typically 0.4 mL) or punishment (air puff) with different probabilities, and were followed by informative Cue2s whose color or texture indicated the trial's outcome (Figure 1A). The non-information-predictive Cue1s also yielded rewards and punishments with matched size and probability, but were followed by noninformative Cue2s whose colors or textures were randomized on each trial and hence did not convey any information about the trial's outcome. The Cue1s were presented in a pseudorandom order in 40-trial blocks of Info and Noinfo trials. We also used a second version of the task in which monkeys were allowed to choose among the Cue1s. Each trial started with the presentation of a trial start cue at the center of the screen. Then, after 1 s, a choice array was presented consisting of two fractals used in the information procedure in Figure 1A. Monkeys then made a saccadic eye movement to their preferred fractal and fixated it for 0.75 seconds to indicate their choice. Then, the unchosen stimulus disappeared, and the exact sequence of events the animals experienced in Figure 1A occurred. Following these trials, during the intertrial interval, another visually distinct fixation spot appeared. When the monkeys fixated this fixation spot, a small reward was delivered (typically, 0.125 mL of juice). This kept the monkeys engaged, particularly when they encountered many trials in which only punishments were available (see Barberini et al., 2012).

QUANTIFICATION AND STATISTICAL ANALYSIS

All statistical tests were two-tailed and non-parametric unless otherwise noted. A significance threshold of $p < 0.05$ was used unless otherwise noted. Recorded neurons were included in analyses if they displayed significant task responsiveness, defined as significant variance in neural activity across all task Cue1s (Kruskal-Wallis test, $p < 0.01$). For this analysis, activity was measured in a broad time window encompassing the task period in order to avoid making any assumptions about the time course of neural responses (from 0.1 s after Cue1 onset to 3.25 s after Cue1 onset).

Neural activity was converted to normalized activity as follows. Each neuron's spiking activity was smoothed with a Gaussian kernel (mean = 50 ms) and then z-scored. To z-score the activity, the neuron's average activity time course aligned at Cue1 onset was calculated for each condition (defined here as each combination of Cue1 and Cue2). These average activity time courses from the different conditions were all concatenated into a single vector, and its mean and standard deviation were calculated and used to z-score the data. Henceforth, all future analyses converted that neuron's firing rates to normalized activity by (1) subtracting the mean of that vector, (2) dividing by the standard deviation of that vector (White et al., 2019).

The Informative Cue Anticipation Index (White et al., 2019) referred to here as the Information Anticipation Index was defined as the difference between a neuron's uncertainty signal for Info and Noinfo trials in a 0.5 s pre-Cue2 time window (Figure 2). Hence the index was positive if a neuron had a higher uncertainty signal in anticipation of Info Cue1s, and negative if a neuron had a higher uncertainty signal in anticipation of Noinfo Cue1s. Neurons were classified as information-responsive if their Information Anticipation Index was significantly different from 0 ($p < 0.05$, permutation tests conducted by comparing the index calculated on the true data to the

distribution of indexes calculated on 20,000 permuted datasets which shuffled the assignment of trials to Info and Noinfo conditions). Exactly as previously, the uncertainty signal was measured by an ROC area comparing certain and uncertain trials, and was computed separately in Info and Noinfo conditions (White et al., 2019).

Analysis of behavioral choice

To model choice behavior, each animal's binary choice data was fit with a logistic regression model. The dependent variable on each trial was the animal's choice (0 or 1 if they chose the leftmost or rightmost option). The regressors were the difference between the right and left options in each specific attribute of the options. The attributes used for the regressors were: the main effects of expected reward value (i.e., reward probability), reward uncertainty (SD of reward distribution), expected punishment (i.e., punishment probability), punishment uncertainty (SD of punishment distribution), informativeness (0 or 1 if the option was non-informative or informative); and the pairwise interactions between informativeness and each of the following variables: expected reward value, reward uncertainty, expected punishment, and punishment uncertainty. In order to obtain regression coefficients in standardized units, all non-binary attributes were standardized by z-scoring before being used to construct the regressors. Thus, their fitted regression weights can be interpreted as increase in the log odds of choosing an option as a result of increasing the option's attribute by an amount equal to one standard deviation of the distribution of that attribute over all options in the task. Finally, to allow for the possibility of interactions between simultaneous expectations of rewarding and aversive outcomes, we modeled the bivalent 50% reward/50% punishment options by setting all of the above attributes to 0 and instead including two additional attributes that were binary indicator variables, one that was 1 if and only if the option was the 50/50 non-informative option, and one that was 1 if and only if the option was the 50/50 informative option. We focused on the Info x Uncertainty terms as measures of each animal's attitudes toward reward and punishment information, as we found that information attitudes were greatly enhanced under uncertainty, such that these terms provided the best explanation of information-related choice behavior (Figure S2). Specifically, when compared to a baseline model in which the only information-related term was a main effect of Info, the model's ability to predict behavior (measured by cross-validated log likelihood assessed by 10-fold cross-validation, by AIC, or by BIC) was improved to a greater extent by adding Info x Uncertainty terms (i.e., Info x Reward Uncertainty and Info x Punishment Uncertainty) than by adding either Info x Probability terms (i.e., Info x Reward Probability and Info x Punishment Probability) or Info x Valence terms (i.e., Info x R and Info x P, where R is an indicator variable equal to 1 when reward is possible and 0 otherwise, and P is an analogous indicator variable for punishment).

Analysis of neural coding prevalence in each neural population

For each animal, area, and outcome type (reward or punishment), we tested whether the fraction of neurons with significant information-anticipatory activity for that outcome type was greater than expected by chance (binomial test, chance = 0.05). Then, for each animal and area, we then classified each neuron as either non-significant or as having one of four coding types: significant reward only, significant aversive only, significant reward and aversive with the same coding sign, and significant reward and aversive with opposite coding signs. We tested whether the fraction of neurons with each coding type was significantly greater than expected under the null hypothesis that no cells had true reward or aversive coding (binomial test, chance = (1-0.05)*0.05 for reward-only and aversive-only and 0.05*0.05*0.5 for same-sign and opposite-signs). Finally, we tested whether, among neurons classified as having one of these four coding types, the fraction of neurons with each coding type was significantly different from that expected under the null hypothesis that neurons had the same probabilities as in the actual data of having significant reward coding and significant aversive coding, but that reward and aversive coding were independent of each other (permutation test, carried out by comparing the observed fraction of neurons with each coding type to the fractions from 1000 permuted datasets in which reward coding and punishment coding properties were each independently shuffled across neurons). We also used these results to perform an analogous test pooling same-sign and opposite-sign neurons to test the overall proportion of cells that anticipated both reward and punishment information, as well as a test based on the difference between the proportions of same-sign and opposite-sign neurons to test whether these neurons had an above-chance tendency to anticipate them with the same sign. We also used an analogous permutation test to determine whether there was a significant difference between vlPFC and ACC in the difference between the proportion of neurons with specific coding properties (e.g., significant reward coding and significant aversive coding with the same sign) and the proportion expected by chance under the null hypothesis of independent coding. Latency of uncertainty and info signals was computed in several ways utilizing previously described methods and produced similar results (Monosov, 2017; Monosov and Hikosaka, 2013; Monosov et al., 2008; White et al., 2019).

Trial-by-trial relationship of activity and Info Anticipation

For the analyses in Figure 4B we calculate the Information Anticipation Index separately using (1) *high-gaze* trials in which the animal gazed at the cue at least 80% of the time in the final 100 ms of the pre-Cue2 window (i.e., a window from 0.9-1.0 s after Cue1 onset) at the location at which Cue2 would be presented and (2) *low-gaze* trials in which the animal gazed at the cue during at most 20% of that time window. We applied this trial selection only to uncertain trials to avoid biasing the index with behavioral differences relative to certain trials. We then visualized the within-neuron difference between these two gaze indices for the population of neurons (Figure 4B). Differences for neurons that displayed negative Information Anticipation Indices (< 0) were sign flipped, so that positive differences indicate that a neuron had greater activity in the same manner that it normally anticipates information (i.e., positive

differences indicate higher activity for cells that were normally excited before information, and indicate lower activity for cells that were normally inhibited before information).

To confirm the robustness of these results, we performed an additional version of this analysis that directly compared neural firing rates between high-gaze versus low-gaze trials, while treating each uncertain punishment condition separately. This is to control for any possibility that the apparent neural-behavioral relationships could be due to mean differences in gaze behavior and/or neural activity across the punishment conditions. To do this, for each neuron, we computed the ROC area for its pre-Cue2 firing rate to discriminate between 'high gaze' and 'low gaze' trials (defined here as trials in which monkeys looked more than 60% of the time versus less than 40% of the time). We computed this separately for each information-predictive Cue1 that was associated with punishment uncertainty, and then averaged these ROC areas to get an overall index of the relationship between that neuron's activity and behavior (Figure 4B, inset). For this analysis we used all neurons with task variability across uncertain punishment conditions, and for each neuron we only used the uncertain punishment conditions where there was behavioral variability while that neuron was recorded, so that the ROC area could be computed.

Analysis of neural activity as a function of gaze state

As a further test of whether information-anticipatory neurons were simply encoding gaze, we directly measured the strength of information-anticipatory activity separately for times during the cue period when the animal's gaze was on the cue versus off the cue. If these neurons were simply encoding gaze state, then information-anticipatory activity should be greatly reduced or abolished after controlling for gaze state, either by restricting the analysis to times when gaze was on the cue *or* to times when gaze was off the cue. Whereas if neurons were truly anticipating information, they should have significant information signals in all cases.

We quantified each neuron's normalized information anticipatory signal using the following procedure, in order to control for the animal's gaze state and the precise time course of neural activity at each millisecond during the cue period. For each neuron and each possible Cue1, we examined each millisecond during the 500 ms pre-Cue 2 period. We found milliseconds where there was at least one trial where the animal was gazing at the cue and one trial where the animal was gazing away from the cue. We then averaged over all such milliseconds to calculate the neuron's mean firing rate for that cue, separately using the gaze on versus gaze off trials. We then quantified the neuron's information anticipatory signal separately for gaze on versus gaze off trials and separately for reward versus punishment outcome types, using the equation: (Rate(info, uncertain outcome) – Rate(Info, certain outcome)) – (Rate(Noinfo, uncertain outcome) – Rate(Noinfo, certain outcome)). We also did an analogous calculation using data from the full 500 ms of the time window using *all* trials regardless of gaze state. We converted these information-anticipatory signals from units of firing rate to normalized firing rate by subtracting the neuron's mean firing rate and dividing by the standard deviation of its firing rate (calculated using the neuron's activity across task conditions in the 500 ms pre-Cue 2 and pre-Outcome time windows), and then sign-normalized by multiplying by the neuron's sign of information coding (i.e., +1 or −1 for cells that were activated or inhibited while anticipating information). Thus, significant information-anticipatory activity in each individual neuron should result in a positive signal.

This control analysis only used the subset of neurons where there was enough variance in gaze behavior that these measures could be computed (i.e., at least one gaze on trial and one gaze off trial for each Info and Noinfo cue with a certain outcome and for at least one pair of Info and Noinfo cues with the same probability of an uncertain outcome). The resulting subset of neurons with significant information-anticipatory activity for reward had highly significantly positive normalized information signals for reward in all cases: when gaze was on the cue, when gaze was off the cue, and when analyzing all data regardless of gaze state ($n = 109$; gaze on, 1.92 ± 0.11, $p < 0.001$; gaze off, 1.78 ± 0.12, $p < 0.001$; all, 1.97 ± 0.09, $p < 0.001$; signed-rank tests). The same was true for the analogous analysis of neurons with significant information-anticipatory activity for punishment ($n = 28$; gaze on, 1.36 ± 0.22, $p < 0.001$; gaze off, 1.25 ± 0.17, $p < 0.001$; all, 1.29 ± 0.12, $p < 0.001$). The same was true for the analogous analysis of neurons with significant information-anticipatory activity for both reward *and* punishment ($n = 10$; reward activity: gaze on, 2.07 ± 0.35, $p = 0.002$; gaze off, 1.89 ± 0.53, $p = 0.002$; all, 2.09 ± 0.35, $p = 0.002$; punishment activity: gaze on, 1.32 ± 0.37, $p = 0.002$; gaze off, 0.98 ± 0.19, $p = 0.002$; all, 1.08 ± 0.19, $p = 0.002$).